

Spectral variation *versus* species β -diversity at different spatial scales: a test in African highland savannas

Duccio Rocchini,^{*a} Kate S. He,^b Jens Oldeland,^{cd} Dirk Wesuls^c and Markus Neteler^a

Received 19th October 2009, Accepted 12th January 2010

First published as an Advance Article on the web 16th February 2010

DOI: 10.1039/b921835a

Few studies exist that explicitly analyse the effect of grain, *i.e.* the sampling unit dimension, on vascular plant species turnover (β -diversity) among sites. While high β -diversity is often a result of high environmental heterogeneity, remotely sensed spectral distances among sampling units may be used as a proxy of environmental gradients which spatially shape the patterns of species turnover. In this communication, we aimed to (i) test the potential relation between spectral variation and species β -diversity in a savanna environment and to (ii) investigate the effect of grain on the achieved patterns. Field data gathered by the BIOTA Southern Africa biodiversity monitoring programme were used to model the relation between spectral variation and species turnover at different spatial grains (10 m \times 10 m and 20 m \times 50 m). Our results indicate that the overall fit was greater at the larger grain size, confirming the theoretical assumption that using a lower grain size would generally lead to a higher noise in the calculation of species turnover. This communication represents one of the first attempts at relating β -diversity to spectral variation, while incorporating the effects of grain size in the study. The results of this study could have significant implications for biodiversity research and conservation planning at a regional or even larger spatial scale.

Introduction

Changes in species composition, *i.e.* the different set of species in different habitats or along gradients of environmental change, represent an important aspect of biodiversity. In fact, species diversity based on community variability is an important proxy of landscape, regional, and global-scale diversity.

However, collecting species data in the field for estimating biodiversity at larger spatial scales can be challenging and unrealistic at times. As stressed by Chiarucci¹ there are a number of issues to be solved before a sampling design may be prepared, such as: (i) the number of sampling units to be investigated in the field, (ii) the choice of spatial placement of the sampling units, (iii) the need to clearly define the statistical population of concern, (iv) the need for an operational definition of a species community, *etc.* Moreover, field-based approaches are often labor intensive and costly, and only a small fraction of a study area may be sampled.^{2,3} Therefore, there is an urgent need to develop robust protocols that effectively sample and monitor biodiversity at various scales. In this view, indirect measures of the environment based on ancillary information such as the variability in climate, soil or in remotely sensed reflectance are powerful tools for locating more diverse areas or at least for guiding field sampling in order to maximise sampling efficiency.³ In particular, remote sensing has long been recognised as the most effective way for predicting species diversity since it can repeatedly allow a synoptic view of an area at regular time intervals.^{4,5}

In species diversity assessment, grain, *i.e.* the size of sampling units, is an important issue since species diversity is strictly related to the area in which species are sampled.^{6–9} However, only few studies exist that explicitly analyse the effect of grain on measures of species turnover, *i.e.* β -diversity which is often a result of environmental heterogeneity.^{10–12} Different methods used to compute β -diversity (see Appendix 1) have been developed over the past decades. Further, a theoretical background on the effect of grain on β -diversity of an area was proposed by Nekola and White,¹⁰ who stated that smaller

^aIASMA Research and Innovation Centre, Fondazione Edmund Mach, Environment and Natural Resources Area, Via E. Mach 1, 38010 S. Michele all'Adige, TN, Italy. E-mail: duccio.rocchini@iasma.it; ducciorocchini@gmail.com; markus.neteler@iasma.it

^bDepartment of Biological Sciences, Murray State University, Murray, Kentucky 42071, USA. E-mail: kate.he@murraystate.edu

^cBiocentre Klein Flottbek & Botanical Garden, University of Hamburg, 22609, Germany. E-mail: oldeland@botanik.uni-hamburg.de; dirk.wesuls@botanik.uni-hamburg.de

^dGerman Aerospace Center, 82203 Oberpfaffenhofen, Germany. E-mail: jens.oldeland@dlr.de

Environmental impact

Remote sensing represents a fascinating tool for species diversity monitoring and it has been widely used in the scientific literature. Nonetheless, it is expected that scale (grain) affects the relationship between species and spectral (*i.e.* environmental) diversity. We aim to: (i) test the potential relation between spectral variation and species β -diversity and (ii) investigate the effect of grain on the achieved patterns.

Our work contributes to an improved knowledge of the relation between species and environmental diversity. In fact, as far as we know, our manuscript represents the first attempt to explicitly account for grain effects on species β -diversity modeling by remotely sensed imagery. The results of this study could provide significant information for facilitating biodiversity research and environmental monitoring.

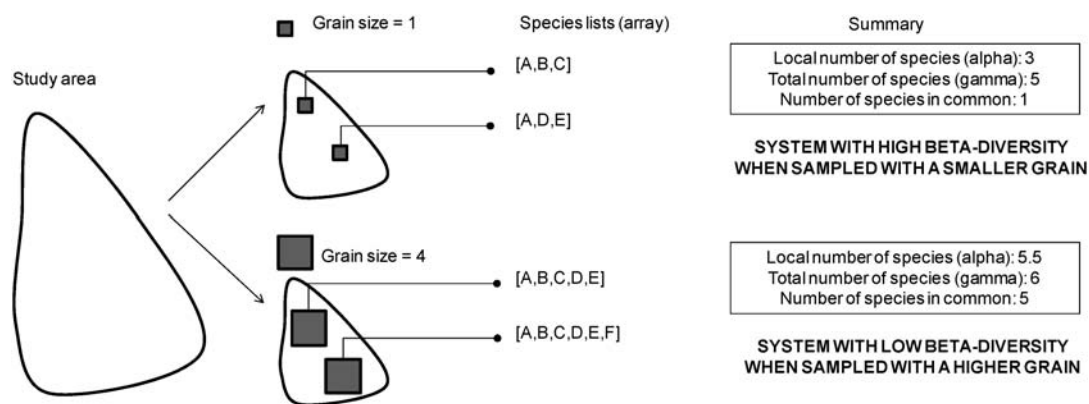


Fig. 1 Grain impact on species inventory. The same study area is sampled by two sampling units. Different grains are considered. Generally, using a smaller grain yields a higher β -diversity in terms of turnover in species composition since smaller sampling units could retain only a part of the whole species pool. However, notice that small sampling units can show (by chance) either higher or lower similarity than the real similarity, introducing a sort of stochastic noise within the input data.

sampling units “will have only a subset of the possible species and will contain identical species lists only a portion of the time”. Hence, it is expected that using smaller sampling units should generally increase the measured β -diversity of an area by decreasing the mean similarity among spatial units. Moreover, smaller sampling units can exhibit (by chance) either higher or lower similarity than the actual similarity, thus introducing a type of stochastic noise within the input data. Fig. 1 presents an example of the concept proposed here.

Despite the importance of this concept, as far as we know, no attempts have been made until now to empirically test this theoretical assumption when modeling species β -diversity by remotely sensed information. Tables 1 and 2 summarise the current efforts made to relate remote sensing data and species diversity, considering both α - (*i.e.* species richness) and β -diversity (*i.e.* species turnover). A huge number of papers have dealt with α -diversity but few of them have considered variations in species composition (hereafter referred to as turnover or β -diversity). Among these, no information has been provided until now about this relation considering different spatial grains.

The aim of this communication is twofold: (i) to test the potential relation between spectral variation derived from remotely sensed imagery as a proxy of regional heterogeneity and species β -diversity in savanna environments and (ii) to investigate the effect of grain on the achieved patterns. It is expected that the results of this study could provide significant information for facilitating biodiversity research and environmental monitoring.

Methods

Study area

The test site, Ovitoto (Longitude: 17° 3' 44.64"E, Latitude 22° 1' 8.76"S) is situated in the Otjozondjupa region in central Namibia, southern Africa (Fig. 2), ranging in elevation from 1500 m to 1600 m above sea level. Climate is semi-arid with an average rainfall of 300–350 mm per year. The main rainy season is summer from December to April, but the rainfall pattern shows a high interannual and spatial variability. The site is a slightly undulating grassy plain with a more or less sparse cover of shrubs (mainly *Catophractes alexandri*). It is dissected by a number of dry riverbeds which are

surrounded by dense thickets of thorny shrubs and small trees (mostly *Acacia* spp.). According to Giess,³³ the area is part of the Namibian Highland savanna. It is used as communal grazing land for cattle and goats by a Herero community.

Field sampling

A 1 km × 1 km test site was established in 2001 as part of the network of the biodiversity observatories belonging to the BIOTA Southern Africa biodiversity monitoring programme (www.biota-africa.org). The area of the square kilometre was subdivided into 100 plots of 1 ha. Twenty 1 ha plots of the 100 available were randomly selected for vegetation monitoring. Every year, plant species composition and cover were recorded in the selected (twenty) plots on different grain sizes: one central 1000 m² plot (20 m × 50 m) and one nested 100 m² plot (10 m × 10 m, Fig. 2). Vegetation data from June 2004 were collected temporally close to the time of the remotely sensed image acquisition (see the following section). Nevertheless, these data were sampled quite late in the respective season, which implies a decline of many short-lived plants. To ensure the best phenological congruence with the remotely sensed data (see next section), vegetation data collected in April 2005 were used in the analysis.

An exploratory analysis on field data was performed in order to check for species β -diversity of the area based on species diversity partitioning³⁴ (see Appendix 1) and species frequency distribution (*e.g.* ref. 35).

Remotely sensed data acquisition and pre-processing

Acquisition of hyperspectral image data from the Ovitoto study area took place in April 2004, using the airborne imaging spectrometer HyMap.³⁶ This sensor measures reflectance in 128 bands covering the 0.44–2.5 μ m spectral region with a spectral bandwidth between 10 and 20 nm. Operational altitude of 3000 m resulted in a spatial resolution of 5 m per pixel. Images have been pre-processed by orthorectifying images using a digital elevation model with a resolution of 30 m × 30 m and ground control points gathered with a differential GPS having a spatial error of only half a metre. Further, an atmospheric calibration using ATCOR4³⁷ was performed in order to remove atmospheric effects that could distort the reflectance signal.

Table 1 Summary of the progress made in modeling α -diversity (*i.e.* species richness) by remote sensing. The table is ordered first by modeling procedure complexity and then by year of the reference. While for community α -diversity (species richness) a large number of papers exist, only a few papers have relied on new methods for estimating or characterising β -diversity (see Table 2)

Species diversity measure and modeling procedure	Study area	Habitat type	Reference
Land cover classification and univariate statistics including species richness per land cover type	Uganda	Tropical forests and wetlands	13
	India	Grassland, evergreen vegetation, savanna	14
Regression between spectral variability or normalized difference vegetation index (NDVI) and species richness for diversity prediction and mapping	Central Canadian Arctic, Canada	Tundra	15
	Tallgrass Prairie Preserve, Oklahoma, US	Grassland	2
	Florida, US	Tropical dry forests	16
	Israel	Mediterranean vegetation	17
Multitemporal NDVI time series and regression analysis for species richness prediction	Central Italy	Wetland	18
	California, US	Chaparral, coastal sage scrub, foothill woodland, and yellow pine forest	19
Remote sensing imagery classification and use of landscape metrics for predicting plant species richness by regression	Kenya	Savanna grasslands and highland moors	20
	Colorado, US	From prairie to tundra	21
Remote sensing classification and geostatistics for mapping species richness	Yucatan, Mexico	Tropical sub-deciduous forests	22
Spectral unmixing of land cover for species richness prediction	Israel	Urban areas	23
Neural networks for species richness prediction	Borneo, Malaysia	Bornean tropical rainforests	24
Multiple regression including remotely sensed information (<i>e.g.</i> land cover) for mapping species richness	Flanders, Belgium	—	25
	Central Italy	Mediterranean vegetation	26
	Switzerland	Alpine vegetation	27
Maximum entropy for species richness mapping	Amazon basin, Northern South America	Amazonian rainforest	28

A minimum noise fraction (hereafter MNF) algorithm was applied in order to reduce dimensionality (by selecting only significant bands) and to filter out noise, which is frequently present in hyperspectral data. MNF consists of two cascading principal component

Table 2 Summary of the progress made in modeling β -diversity (*i.e.* species turnover) by remote sensing. The table is ordered first by modeling procedure complexity and then by year of the reference

Species diversity measure and modeling procedure	Study area	Habitat type	Reference
Correlations (measured with the Mantel test) of floristic similarities with spectral similarities	Ecuador	Amazonian rainforest	29
Correlations of plant species turnover and spectral variation at different taxonomic ranks	North and South Carolina, USA	Forests, grasslands	30
Correlation between β -diversity and differences in productivity among global ecoregions, biomes, and biogeographical realms	Worldwide	WWF-based ecoregions	31
Quantile regression applied to the distance decay of species similarity <i>versus</i> spectral distance	Central Italy	Mediterranean vegetation	32

transformations, with a noise whitening step, refer to Green *et al.*³⁸ for additional information on MNF's mathematical details. The MNF eigenvalues can be used to determine the inherent dimensionality of the data set.

The magnitude of each eigenvalue is an indicator of the amount of original scene information content that is captured in its corresponding MNF component. Eigenvalues smaller than one are said to be capturing only noise. To choose the optimal number of MNF components, it is a general rule of thumb to apply a threshold around one while interpreting a scree plot of the eigenvalues. The majority of information was retained in the first ten MNF-derived components (EV > 2) which were used for further analysis. Image analysis was performed using ENVI 4.2.

Modeling species *versus* spectral variation

Turnover in species composition (β -diversity) between pairs of plots was calculated at the two considered grains (10 m × 10 m and 20 m × 50 m) based on the Sørensen coefficient (C_s , see Appendix 1), on the strength of its widespread use (see *e.g.* ref. 39 and 40 for details on species compositional metrics and Appendix 1 for the formula used). At the same time, for each plot (at both grains, 10 m × 10 m and 20 m × 50 m) the mean spectral value for each MNF band (10 dimensions) was extracted considering those pixels falling therein and a semi-matrix of pair-wise distances between plots was derived

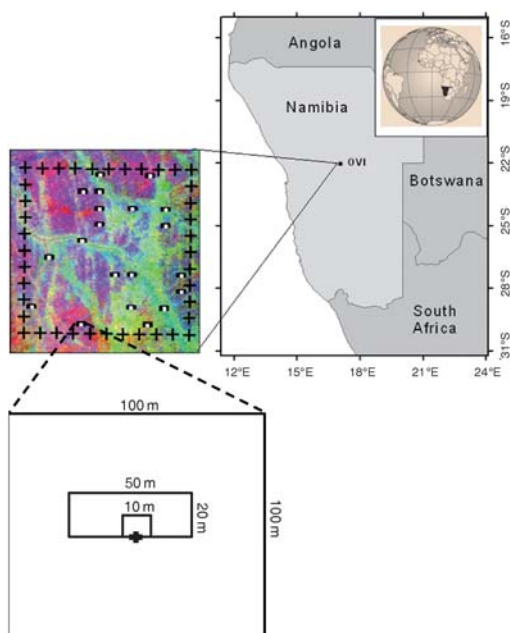


Fig. 2 Study area: the Ovitoto test site (central Namibia, Africa) of 1×1 km (black crossed area overlapped on the HyMap hyperspectral image, first 3 MNF bands in RGB) where plant species composition was sampled. The area was firstly divided into 100 one-hectare squares and twenty out of these were randomly selected and sampled using $20 \text{ m} \times 50 \text{ m}$ and $10 \text{ m} \times 10 \text{ m}$ sampling units. Refer to the main text for major information.

based on the spectral Euclidean distance. Refer to Appendix 2 for the background of spectral variation measurement.

The correlation between species turnover and spectral variation was assessed by Pearson correlation coefficient. A linear model was fitted in order to estimate the rate (based on the slope and intercept) of species change *versus* spectral variation. A statistical test was performed using 999 Monte Carlo permutations. Monte Carlo permutation was applied in order to solve the false number of degrees of freedom created by distance-based models (in this case, having $N = 20$ sampling units, $df = (N \times (N - 1)/2) - 2 = 188$, see ref. 8, 29, and 30).

Results

A total of 98 and 138 vascular plant species were found in the twenty sampling units at the $10 \text{ m} \times 10 \text{ m}$ and $20 \text{ m} \times 50 \text{ m}$ grain sizes, with a mean amount of species per plot (α -diversity) equaling 18.4 (SD 8.62) and 40.95 (SD 11.2), respectively. Using the additive partitioning of diversity (see Appendix 1), β -diversity was determined to be 79.6 (*i.e.* the 81.22% of total γ -diversity) and 90.05 (*i.e.* the 68.74% of total γ -diversity). Hence, a high amount of species turnover was found in the area using both grain sizes.

This was further demonstrated by the frequency distribution of the species occurring in the plots at the $10 \text{ m} \times 10 \text{ m}$ and $20 \text{ m} \times 50 \text{ m}$ scales respectively. In both cases, most of the species occurred in very few plots (*e.g.* only one plot) while very few species were present in all the plots sampled (Fig. 3).

Most importantly, positive relationships between β -diversity and spectral variation were found at both grain sizes ($p < 0.01$) (Fig. 4). The slope was the same for both grain sizes but the smaller grain

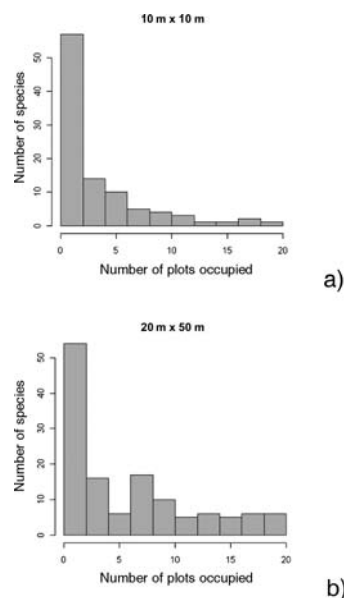


Fig. 3 Frequency distribution of species considering different spatial grains: (a) $10 \text{ m} \times 10 \text{ m}$; (b) $20 \text{ m} \times 50 \text{ m}$.

produced a greater range in species turnover values, evident as much higher scatter in Fig. 4a compared to Fig. 4b. This led to a lower correlation coefficient considering the $10 \text{ m} \times 10 \text{ m}$ ($R = 0.374$, $p < 0.01$) rather than the $20 \text{ m} \times 50 \text{ m}$ ($R = 0.443$, $p < 0.01$) spatial grains.

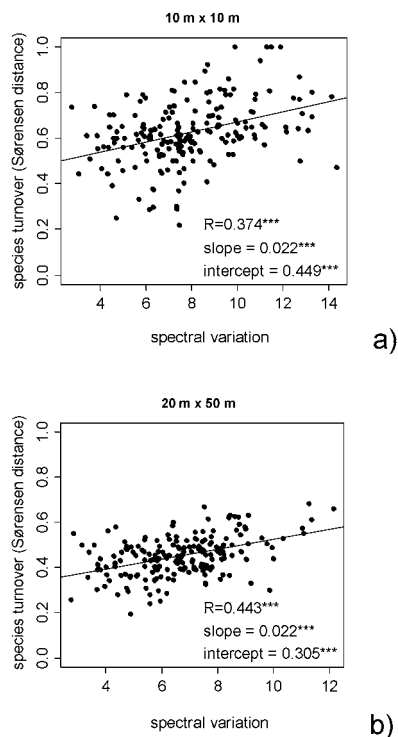


Fig. 4 Species turnover measured by the Sørensen distance between pair-wise plots *versus* spectral variation measured by the Euclidean spectral distance among plots, considering different spatial grains: (a) $10 \text{ m} \times 10 \text{ m}$; (b) $20 \text{ m} \times 50 \text{ m}$.

Lastly, the intercept of the fitted linear models equaled 0.449 and 0.305 at the 10 m × 10 m and 20 m × 50 m, *i.e.* a higher species turnover was found at lower grain size even with very similar habitat conditions.

Discussion

Although two relatively fine grains were examined in this study (100 m² and 1000 m²), our findings support the generality that the overall fit improves at a larger spatial window of analysis. In other words, we confirmed the theoretical assumption that using a lower grain size would generally lead to a higher noise in the data sampled as found by Nekola⁴¹ for plant communities in north-east Iowa. Similar results were also attained by Steinitz *et al.*¹² who related snail species and rainfall variation among plots at different grain sizes, finding that data taken at smaller grain sizes showed a weaker correlation between species similarity and rainfall distance since increasing the grain size could average the local stochastic variation in species composition.

The same concept applies to the results achieved in this communication where smaller grain sizes led to a lower correlation between species turnover and spectral variation due to a higher stochastic variability in species dissimilarities when using smaller grain sizes.¹⁰ Moreover, the intercept values attained in this study, representing the amount of species turnover with no spectral differences, demonstrate that even areas which are ecologically similar will share few species when using smaller grains.

However, despite the theoretical and empirical evidence of the effect of grain size on species turnover measurement, the problem is rarely accounted for (*e.g.* ref. 11). As an example, quoting Soininen *et al.*⁴² who performed a meta-analysis on the matter, “most of the studies included [in the meta-analysis] do not show detailed information on the grain of the study”, hence weakening the capability of accounting for grain effects on β -diversity measurement leading to contrasting, misleading or non-comparable results among studies.

The savanna environment surveyed in this communication represents a relatively suitable ecosystem for testing the proposed method, as the vegetation structure varies from open grassland to patches with high canopy cover of shrubs, promoting a high β -diversity.

In forest ecosystems, on the other hand, the spatial heterogeneity perceived by the remote sensor could be lower because of a potentially similar canopy cover.⁵ However, the structure of the canopy layers could reveal the heterogeneity related to forest structure and diversity, providing useful results, especially in ecosystems with a very high degree of fragmentation. This is especially true when using a hyperspectral sensor like HyMap instead of multispectral images.⁴³ In fact, hyperspectral imagery may better discern among different vegetation types hence being more suitable even with respect to very high spatial resolution imagery. The availability of data with improved spatial and (overall) spectral resolutions represents an opportunity for studies of the relationship between spectral and ecological heterogeneity.⁴⁴ In this view, high spectral resolution is particularly desired since measuring ecological distance among sites using a larger bandwidth may be crucial for finding ecological gradients shaping species diversity.

Conservation decisions are often taken despite incomplete information.⁴⁵ As previously stated, in some cases species lists are not available since they are time consuming to collect²³ or study areas are

unattainable,⁴⁶ while spectral data from optical remotely sensed imagery are directly available synoptic over large areas.⁴⁷ Spectral distance represents a direct effect of environmental properties thus representing a powerful tool for gradient analysis.²⁹ Hence, knowing *a priori* areas with higher ecological heterogeneity using spectral distance may become crucial for species diversity estimation and conservation planning. Methods utilising remotely sensed optical characteristics can provide important information on the dynamics of the compositional features of plant communities in a given area. At the same time, it should also be stressed that the achieved results should be viewed as a helpful guideline for planning field survey rather than a replacement of it, limiting remotely sensed information as a driver only for optimised field sampling design strategies.

Moreover, in this study, we did not make use of classified land use maps in order to detect ecological gradients but we relied directly on spectral distances based on the fact that spectral variation may be directly related to ecological variability. We consider that spectral data is a better proxy of ecological gradients than the classified maps and agree with the suggestion of Palmer *et al.*² that processing and classifying images can result in an important loss of information, due to the degradation of continuous quantitative information into discrete classes.

Appendix 1. Basic measures of β -diversity

While alpha (α) and gamma (γ) diversities rely only on the number of species at local and global scales (respectively), accounting for species turnover may allow differences in species composition to be accounted for.

A first attempt to quantitatively define β -diversity (β) was that of Whittaker⁴⁸ who expressed it as:

$$\beta = \frac{\gamma}{\alpha} \quad (1)$$

with γ = total species richness over a study area.

This was later modified by Lande³⁴ into an additive partitioning as (see ref. 34 and 49):

$$\gamma = \alpha + \beta \quad (2)$$

leading to considering β in the same unit of measurement (*i.e.* number of species) of α and γ diversities as:

$$\beta = \gamma - \alpha \quad (3)$$

Given N sampling units, these approaches will return one single index of β -diversity.

On the other hand, computing β -diversity by looking at the differences between pairs of plots in terms of species composition would allow the building of semimatrices which show the diversity between each pair of plots.^{50,51} This latter approach has been used in this communication.

Popular indices of β -diversity, *e.g.* the Jaccard (C_j) or the Sørensen (C_s) indices, basically rely on the theory of sets where the intersection of the composition in species between pairs of plots (*i.e.* the intersection of two sets: \cap) is compared to their union (\cup , see ref. 48), according to the following formulas:

$$C_j = \frac{j}{a + b + j} \quad (4)$$

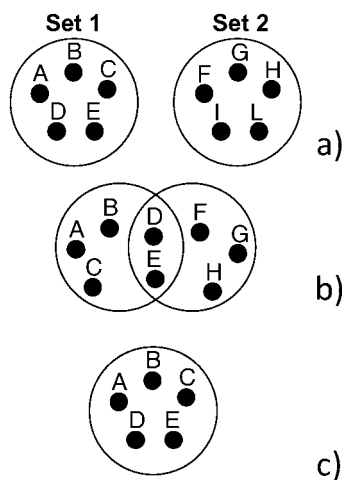


Fig. 5 Given 2 sets (sampling units) with *e.g.* 5 elements (species) β -diversity will range from 0 to 1 when the sets share no or all species, respectively. (a) Highest β -diversity case, no species are shared by the two sampling units, (b) intermediate β -diversity, some of the species are shared, and (c) lowest β -diversity, all species are shared by the two sampling units. A similar example is provided by Chao *et al.*⁵⁰

$$C_s = \frac{2j}{a + b + 2j} \quad (5)$$

where j = number of species shared by plots (sets) 1 and 2; a = number of unique species of plot 1; b = number of unique species of plot 2, the Jaccard (C_j) and Sørensen (C_s) indices accounting for the overlap between two species lists and ranging from 0, indicating perfect dissimilarity, to 1, indicating perfect similarity.

The higher the intersection in species composition the lower the β -diversity. Hence, β -diversity measured by C_j or C_s turns out to be $\beta_{C_j} = 1 - C_j$ and $\beta_{C_s} = 1 - C_s$, ranging from zero (complete intersection between sets) to 1 (no intersection between sets).

As an example, consider two sets (sampling units) with the same number of elements (species) therein (α -diversity = 5). Using the Jaccard or the Sørensen index, β -diversity will range from 0, when the 5 species will be exactly the same, to 1, when all the 5 species will be different. Fig. 5 helps illustrating the problem.

The system represented in Fig. 5a has the highest β - and γ -diversity since, given the same α -diversity (equaling 5), no species are shared. The diversity D of the system turns out to be:

$$D = \begin{cases} \alpha = 5 \\ \gamma = 10 \\ \beta_{C_j} = 1 - C_j = 1 \quad \text{or} \quad \beta_{C_s} = 1 - C_s = 1 \end{cases} \quad (6)$$

The situation of Fig. 5b has an intermediate β (and thus γ) diversity since two of the five species of each site are shared. Hence, the diversity D of the system turns out to be:

$$D = \begin{cases} \alpha = 5 \\ \gamma = 8 \\ \beta_{C_j} = 1 - C_j = 0.75 \quad \text{or} \quad \beta_{C_s} = 1 - C_s = 0.6 \end{cases} \quad (7)$$

Finally, in the last case (Fig. 5c), the two sets share all their elements. Thus α -diversity coincides with γ -diversity and β -diversity decreases to zero, as:

$$D = \begin{cases} \alpha = 5 \\ \gamma = 5 \\ \beta_{C_j} = 1 - C_j = 0 \quad \text{or} \quad \beta_{C_s} = 1 - C_s = 0 \end{cases} \quad (8)$$

It is far beyond the aim of this communication to compare different kinds of β -diversity measures. The Sørensen index was used on the strength of its widespread use (see *e.g.* ref. 39 and 40).

Appendix 2. Measuring spectral variation between pairs of plots

Consider a remotely sensed image composed by N bands. Once minimum noise fraction (MNF, see ref. 38) has been performed the resulting image will be composed by a number $N_{\text{MNF}} < N$ bands. In this theoretical example we set $N = 10$ reduced by MNF to $N_{\text{MNF}} = 3$ (Fig. 6).

Once the MNF image has been superimposed on the field sampling units, pixels laying within each sampling unit can be extracted.

Then, each sampling unit may be represented as a cloud of points within a spectral space defined by the MNF bands as axes (Fig. 6). In this example, the spectral space is three-dimensional for graphical reasons but indeed a N_{MNF} -dimensional spectral space is used, where N_{MNF} equals to the number of MNF-derived bands.

Measuring the Euclidean distance in the MNF spectral space between clouds will correspond to the spectral distance (*i.e.* variation) between pair-wise plots. Many distance measures may be used but the

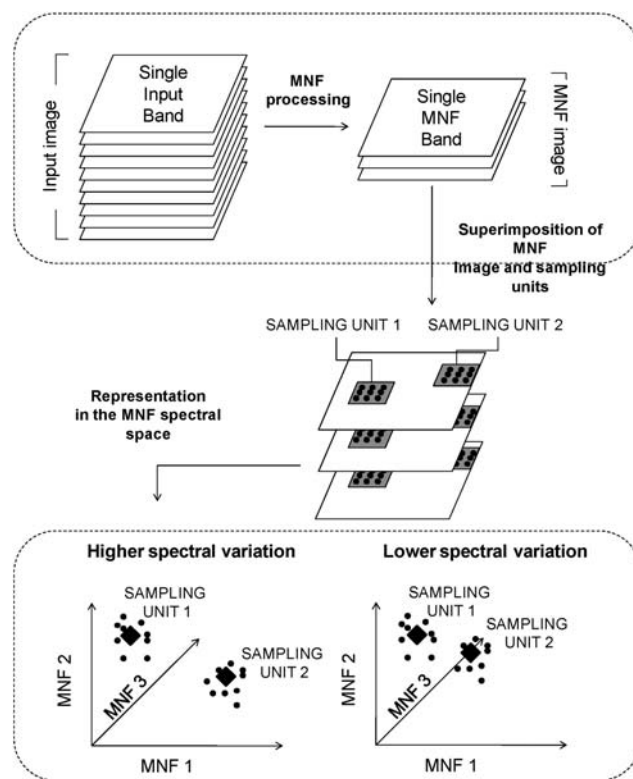


Fig. 6 Schematic representation of the spectral variation measurement considering two sampling units. Refer to the main text of the Appendix 2 for detailed information. Notice that pixels are represented as points for graphical clarity.

most common is based on the centroid to centroid Euclidean distance. The spectral centroid (diamond in Fig. 6) is defined as the point having as spectral coordinates the mean spectral value of the cloud of points^{2,18} in each MNF band.

Two different situations are represented in Fig. 6. In the first one, spectral centroids are more distant from each other. Hence there is a higher spectral variation. Instead, in the second case, spectral centroids are near to each other. Thus, spectral variation would be low.

A higher spectral variation is expected to be related to a higher ecological heterogeneity and thus to a higher β -diversity (see Appendix 1).

Acknowledgements

We are grateful to two anonymous reviewers for suggestions on a previous version of the manuscript. We thank Lena Lieckfeld and Dr Martin Bachmann for image processing and helpful comments on hyperspectral imagery, Helmholtz-EOS (www.helmholtz-eos.de) and the German Federal Ministry for Education and Research funded this project (01LC0624A2).

Notes and references

- 1 A. Chiarucci, *Folia Geobot.*, 2007, **42**, 209–216.
- 2 M. W. Palmer, P. Earls, B. W. Hoagland, P. S. White and T. Wohlgemuth, *Environmetrics*, 2002, **13**, 121–137.
- 3 D. Rocchini, S. Andreini Butini and A. Chiarucci, *Global Ecol. Biogeogr.*, 2005, **14**, 431–437.
- 4 D. M. Stoms and J. E. Estes, *Int. J. Remote Sens.*, 1993, **14**, 1839–1860.
- 5 H. Nagendra, *Int. J. Remote Sens.*, 2001, **22**, 2377–2400.
- 6 O. Arrhenius, *J. Ecol.*, 1921, **9**, 95–99.
- 7 R. H. MacArthur and E. O. Wilson, *The theory of Island Biogeography*, Princeton University Press, Princeton, 1967.
- 8 P. Legendre and L. Legendre, *Numerical Ecology*, Elsevier Science BV, Amsterdam, 2nd English edn, 1998.
- 9 G. Bacaro, E. Baragatti and A. Chiarucci, *J. Environ. Monit.*, 2009, **11**, 798–801.
- 10 J. C. Nekola and P. S. White, *J. Biogeogr.*, 1999, **26**, 867–878.
- 11 M. Vellend, *J. Veg. Sci.*, 2001, **12**, 545–552.
- 12 O. Steinitz, J. Heller, A. Tsoar, D. Rotem and R. Kadmon, *J. Biogeogr.*, 2006, **33**, 1044–1054.
- 13 R. M. Fuller, G. B. Groom, S. Mugisha, P. Ipulet, D. Pomeroy, A. Katende, R. Bailey and R. Ogutu-Ohwayo, *Biol. Conserv.*, 1998, **86**, 379–391.
- 14 H. Nagendra and M. Gadgil, *Proc. Natl. Acad. Sci. U. S. A.*, 1999, **96**, 9154–9158.
- 15 W. Gould, *Ecol. Appl.*, 2000, **10**, 1861–1870.
- 16 T. W. Gillespie, *Ecol. Appl.*, 2006, **15**, 27–37.
- 17 N. Levin, A. Shmida, O. Levanoni, H. Tamari and S. Kark, *Divers. Distrib.*, 2007, **13**, 692–703.
- 18 D. Rocchini, *Remote Sens. Environ.*, 2007, **111**, 423–434.
- 19 D. H. K. Fairbanks and K. C. McGwire, *Global Ecol. Biogeogr.*, 2004, **13**, 221–235.
- 20 B. O. Oindo and A. K. Skidmore, *Int. J. Remote Sens.*, 2002, **23**, 285–298.
- 21 S. Kumar, T. J. Stohlgren and G. W. Chong, *Ecology*, 2006, **87**, 3186–3199.
- 22 J. L. Hernandez-Stefanoni and J. Dupuy, *Biodivers. Conserv.*, 2007, **16**, 3817–3833.
- 23 G. Bino, N. Levin, S. Darawshi, N. van der Hal, A. Reich-Solomon and S. Kark, *Int. J. Remote Sens.*, 2008, **29**, 3675–3700.
- 24 G. M. Foody and M. E. J. Cutler, *J. Biogeogr.*, 2003, **30**, 1053–1066.
- 25 O. Honnay, K. Piessens, W. Van Landuyt, M. Hermy and H. Gulinck, *Landsc. Urban Plann.*, 2003, **63**, 241–250.
- 26 G. Bacaro, D. Rocchini, I. Bonini, M. Marignani, S. Maccherini and A. Chiarucci, *Plant Biosystems*, 2008, **142**, 630–642.
- 27 T. Wohlgemuth, M. P. Nobis, F. Kienast and M. Plattner, *J. Biogeogr.*, 2008, **35**, 1226–1240.
- 28 S. Saatchi, W. Buermann, H. ter Steege, S. Mori and T. B. Smith, *Remote Sens. Environ.*, 2008, **112**, 2000–2017.
- 29 H. Tuomisto, A. D. Poulsen, K. Ruokolainen, R. C. Moran, C. Quintana, J. Celi and G. Cañas, *Ecol. Appl.*, 2003, **13**, 352–371.
- 30 K. S. He, J. Zhang and Q. Zhang, *Acta Oecol.*, 2009, **35**, 14–21.
- 31 K. S. He and J. Zhang, *Ecol. Inform.*, 2009, **4**, 93–98.
- 32 D. Rocchini and B. S. Cade, *IEEE Geosci. Remote Sens. Lett.*, 2008, **5**, 640–643.
- 33 W. Giess, *Dinteria*, 1971, **4**, 1–114.
- 34 R. Lande, *Oikos*, 1996, **76**, 5–13.
- 35 M. McGeoch and K. J. Gaston, *Biol. Rev.*, 2002, **77**, 311–331.
- 36 T. Cocks, R. Janssen, A. Stewart, I. Wilson and T. Shields, *1st EARSEL Workshop on Imaging Spectroscopy*, Zurich 1–7, 1998.
- 37 R. Richter and D. Schläpfer, *Int. J. Remote Sens.*, 2002, **23**, 2631–2649.
- 38 A. A. Green, M. Berman, P. Switzer and M. D. Craig, *IEEE Trans. Geosci. Remote Sens.*, 1988, **26**, 65–74.
- 39 M. W. Wilson and A. Schmida, *J. Ecol.*, 1984, **72**, 1055–1064.
- 40 P. Koleff, K. J. Gaston and J. J. Lennon, *J. Anim. Ecol.*, 2003, **72**, 367–382.
- 41 J. C. Nekola, *Ecology*, 1999, **80**, 2459–2473.
- 42 J. Soinenen, R. McDonald and H. Hillebrand, *Ecography*, 2007, **30**, 3–12.
- 43 J. Oldeland, D. Wesuls, D. Rocchini, M. Schmidt and N. Jürgens, *Ecol. Indic.*, 2010, **10**, 390–396.
- 44 H. Nagendra and D. Rocchini, *Biodivers. Conserv.*, 2008, **17**, 3431–3442.
- 45 S. Polasky, J. D. Camm, A. R. Solow, B. Csuti, D. White and R. Ding, *Biol. Conserv.*, 2000, **94**, 1–10.
- 46 J. M. Read, D. B. Clark, E. M. Venticinque and M. P. Moreiras, *J. Appl. Ecol.*, 2003, **40**, 592–600.
- 47 T. W. Gillespie, G. M. Foody, D. Rocchini, A. P. Giorgi and S. Saatchi, *Progr. Phys. Geogr.*, 2008, **32**, 203–221.
- 48 R. Whittaker, *Taxon*, 1972, **21**, 213–251.
- 49 T. O. Crist and J. A. Veech, *Ecol. Lett.*, 2006, **9**, 923–932.
- 50 A. Chao, R. L. Chazdon, R. K. Colwell and T.-J. Shen, *Ecol. Lett.*, 2005, **8**, 148–159.
- 51 G. Bacaro and C. Ricotta, *Community Ecol.*, 2007, **8**, 41–46.